Journal of the American Heart Association

ORIGINAL RESEARCH

Comparative Analysis of Blood-Derived Endothelial Cells for Designing Next-Generation Personalized Organ-on-Chips

Tanmay Mathur, MTech; James J. Tronolone, MS; Abhishek Jain, PhD

BACKGROUND: Organ-on-chip technology has accelerated in vitro preclinical research of the vascular system, and a key strength of this platform is its promise to impact personalized medicine by providing a primary human cell–culture environment where endothelial cells are directly biopsied from individual tissue or differentiated through stem cell biotechniques. However, these methods are difficult to adopt in laboratories, and often result in impurity and heterogeneity of cells. This limits the power of organ-chips in making accurate physiological predictions. In this study, we report the use of blood-derived endothelial cells as alternatives to primary and induced pluripotent stem cell–derived endothelial cells.

METHODS AND RESULTS: Here, the genotype, phenotype, and organ-chip functional characteristics of blood-derived outgrowth endothelial cells were compared against commercially available and most used primary endothelial cells and induced pluripotent stem cell–derived endothelial cells. The methods include RNA-sequencing, as well as criterion standard assays of cell marker expression, growth kinetics, migration potential, and vasculogenesis. Finally, thromboinflammatory responses under shear using vessel-chips engineered with blood-derived endothelial cells were assessed. Blood-derived endothelial cells exhibit the criterion standard hallmarks of typical endothelial cells. There are differences in gene expression profiles between different sources of endothelial cells, but blood-derived cells are relatively closer to primary cells than induced pluripotent stem cell–derived. Furthermore, blood-derived endothelial cells are much easier to obtain from individuals and yet, they serve as an equally effective cell source for functional studies and organ-chips compared with primary cells or induced pluripotent stem cell–derived cells.

CONCLUSIONS: Blood-derived endothelial cells may be used in preclinical research for developing more robust and personalized next-generation disease models using organ-on-chips.

Key Words: blood outgrowth endothelial cells ■ experimental cell model ■ organ-on-chip ■ vascular bioengineering

Cardiovascular complications are the leading causes of patient morbidity and mortality worldwide.[1,2] Patients also exhibit significant heterogeneity in the pathological manifestation of the diseases, further exacerbating the clinical burden.[3,4] Different patients show different extents of clinical severity of the disease. Hence, developing therapeutic strategies against such a diverse phenotype has been difficult and the "one-size-fits-all" approach cannot meet the current clinical needs. Recently engineered microphysiological organ-chip or vessel-chip platforms have garnered significant interest in the past decade as an effective vascular disease modeling and drug screening tool by clinicians and pharmaceutical agencies.[5,6] Organ-chips offer amalgamation of crucial tissue microenvironments with relevant biological and pathological factors that allow researchers to mimic the cellular/tissue level interactions observed in pathophysiological conditions.[7,8] However, current organ-chips still lack the inclusion of a phenotypically relevant

Correspondence to: Abhishek Jain, PhD, Department of Biomedical Engineering, Texas A&M College of Engineering, 101 Bizzell St, College Station, TX 77843. E-mail: a.jain@tamu.edu

Supplementary Material for this article is available at https://www.ahajournals.org/doi/suppl/10.1161/JAHA.121.022795

For Sources of Funding and Disclosures, see page 13.

JAHA is available at: www.ahajournals.org/journal/jaha

CLINICAL PERSPECTIVE

What Is New?

- Organ-on-chip technology has accelerated in vitro preclinical research of the vascular system; however, these models lack the inclusion of patient-derived cells, which limits the power of organ-chips in making accurate physiological predictions.
- This study provides evidence that blood-derived endothelial cells are suitable patient-specific alternatives to commercially available primary endothelial cells and induced pluripotent stem cell–derived endothelial cells.

What Are the Clinical Implications?

- Blood-derived endothelial cells can be used in preclinical research for developing more robust and personalized next-generation disease models using organ-on-chips.

Nonstandard Abbreviations and Acronyms

BOECs	blood outgrowth endothelial cells
HUVECs	human umbilical vein endothelial cells
iPSCs	induced pluripotent stem cells
iPSC-ECs or iECs	induced pluripotent stem cell–derived endothelial cells
KEGG	Kyoto Encyclopedia of Genes and Genomes
NHLFs	normal human lung fibroblasts

patient-derived tissue source and hence cannot predict the significant patient-to-patient variability observed clinically within the diseases. Current vessel-chip platforms have depended on using primary endothelial cells (ECs) such as human umbilical vein endothelial cells (HUVECs), which are often obtained from pooled individual sources and require exogenous stimulation through cytokines or other inflammatory agents to induce a pathological state.[9,10] Alternatively, induced pluripotent stem cell derived endothelial cells (iPSC-ECs or iECs)[11,12] derived from patients are an emerging class of cells being incorporated in organ-chip techniques, but the current methods of isolating and differentiating cells is time-consuming and requires highly sophisticated skills to obtain a phenotypically pure cell type.[13] These differentiation protocols are also sensitive to the growth/differentiation factors and their time of administration, making them less suitable for use in low resource or clinical settings where specialized technicians might not be available.[14]

Recently, our group identified an alternative endothelial cell source that is patient blood derived that can be cultured in microfluidic devices.[15,16] These blood-derived endothelial cells or blood outgrowth endothelial cells (BOECs) are suggested as endothelial progenitor cells found in blood that have differentiated into a mature endothelial cell type.[17] Isolation of BOECs from patients requires simple density gradient centrifugation and colonies start appearing within 2 weeks of plating.[16] Compared with deriving other autologous cell sources such as tissue biopsies for primary cells or iPSC-derived endothelial cells, BOECs isolation and expansion is relatively easier and straightforward without the need for highly trained individuals or expensive reagents (Figure 1).[18–21]

Our objective in this work was to investigate how these cells compare to primary cells such as HUVECs and other patient-derived cells such as iECs. In this study, we report the phenotypic and transcriptomic differences in the microphysiological behavior of primary HUVECs, iECs, and BOECs. BOECs are compared on their expression of pro-endothelial markers, blood vessel formation in vitro, growth kinetics and migration, response to fluid shear stress, response to cytokine stimulation, and thromboinflammation after whole blood perfusion. We also compare the transcriptomic profiles of BOECs with HUVECs and iECs through next-generation RNA sequencing and differential gene expression analysis. Finally, our outcomes with vessel-chip analysis confirm that blood-derived endothelial cells such as BOECs can be used across the organ-on-chip research platforms requiring generic or patient-specific primary vascular cells.

METHODS

Data Availability

The data that support the findings of this study are available from the corresponding author upon reasonable request. The RNA sequencing data reported in this article have been deposited in the Gene Expression Omnibus (GEO) database, https://www.ncbi.nlm.nih.gov/geo (accession no, GSE184791).

Cell Culture and BOEC Isolation

HUVECs and iECs were purchased from Lonza and Fujifilm Cellular Dynamics International (iCell Endothelial Cells 11713, FCDI), respectively. HUVECs were cultured in endothelial growth media 2 (EGM2, PromoCell) and used until passage 8. iECs were cultured in VascuLife VEGF Endothelial Media supplemented with iCell Endothelial Cells Medium Supplement (FCDI) and used

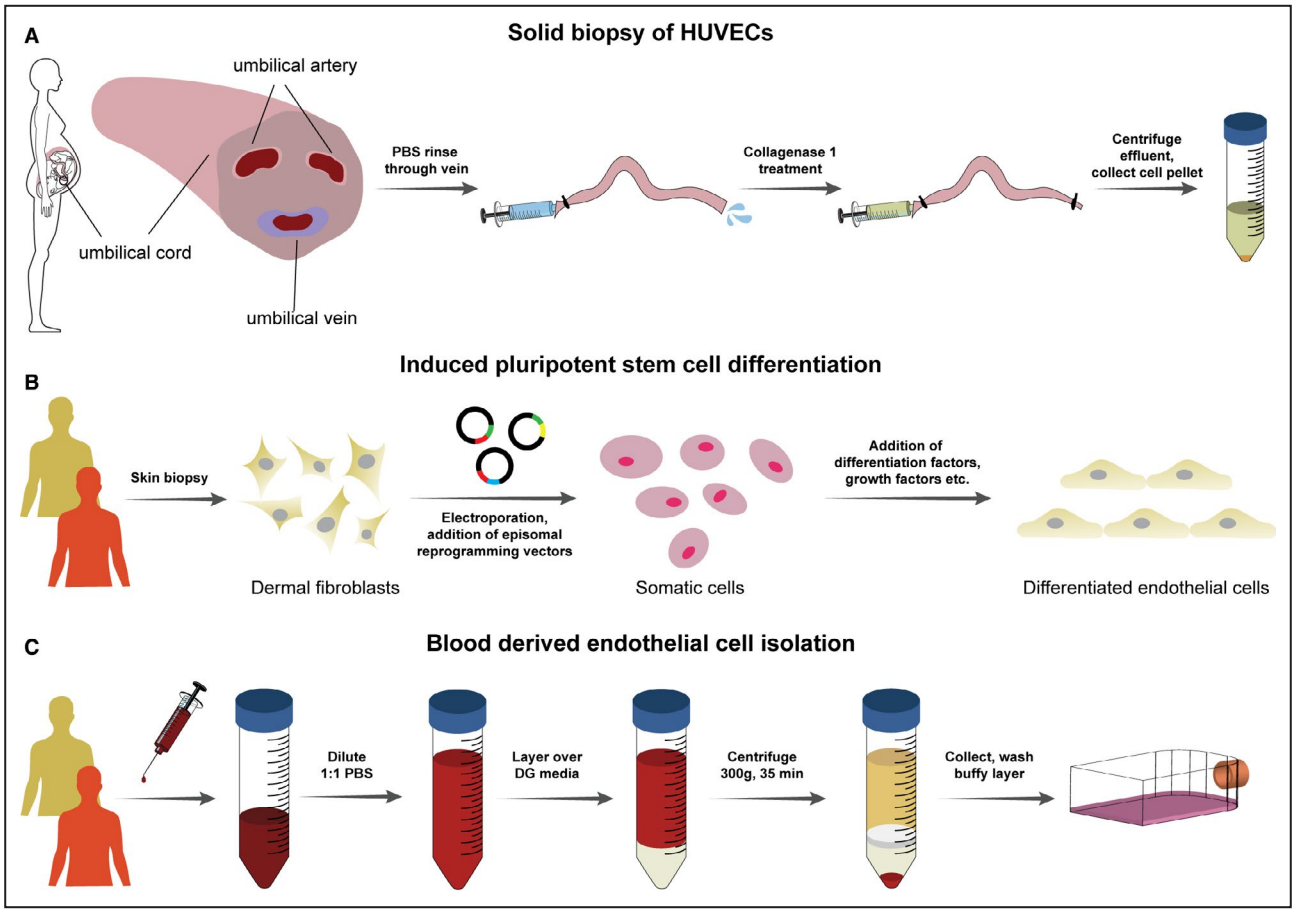

Figure 1. Common methods for isolation/differentiation of primary human endothelial cells.
A, Schematic of the HUVEC extraction protocol. Umbilical veins from the discarded umbilical cords are washed with PBS and perfused with a cleaving agent such as collagenase I to remove adherent endothelial cells. The suspension is then collected and centrifuged to collect HUVECs, which can be cultured in tissue culture flasks.[18,20] **B**, Schematic of the iPSC differentiation and subsequent induction of endothelial differentiation protocol. Dermal fibroblasts or blood cells are reprogrammed into pluripotency using either lentiviral vectors or integration free episomal vectors. The reprogrammed somatic cells are then differentiated into endothelial subtypes after addition of growth factors such as VEGF, FGF, etc, and culturing in endothelial growth media.[19,21] The reprogramming and differentiation require 3–4 weeks to obtain functionally pure endothelial cells through sorting. **C**, Schematic of BOEC isolation procedure. Whole blood from donors is mixed with equal volumes of PBS and centrifuged after layering over density gradient medium. The buffy layer is separated and plated onto tissue culture flasks containing endothelial growth media. Colonies of endothelial cells appear 2–3 weeks after plating. BOEC indicates blood outgrowth endothelial cell; DG, density gradient; FGF, fibroblast growth factor; HUVECs, human umbilical vein endothelial cell; iPSC, induced pluripotent stem cell; PBS, phosphate-buffered saline; and VEGF, vascular endothelial growth factor.

until passage 5 as per manufacturer's protocol. BOECs were isolated from healthy whole blood samples according to the protocol published by our group.[15,16] BOECs were cultured in collagen-coated tissue culture flasks with endothelial growth media supplemented with 10% FBS (Gibco) and used until they reached passage 8. Media was replaced every 48 hours until all cells reached 80% confluence. All cells were subcultured and re-plated at seeding density of 15 000 cells/cm^2 and incubated in a 5% CO_2 incubator at 37 ˚C.

Flow Cytometry

Pelleted cells were fixed with 4% paraformaldehyde (Thermo) for 15 minutes. The cells were then centrifuged again and the cell pellet was resuspended in the respective antibody solutions (1:100 dilution in 1X PBS) and incubated for an hour at room temperature. After the incubation, the cells were centrifuged and re-suspended in 1X PBS. For each cell type and marker of interest, 10 000 cells were analyzed.

Migration Assay

Cells cultured in 24-well plates were formed into confluent monolayers and then, a 200-µL pipette tip (P200, Genesee Scientific) was used to create a ≈1-mm linear scratch. The cells that got detached were aspirated after washing the wells with 1X PBS twice. The PBS was finally replaced with EGM2 for all cells,

and images of the scratch healing process were taken every 8 hours. Images were the analyzed in ImageJ/Fiji and wound healing was reported as percent area recovered.

Microvascular Self-Assembly (Vasculogenesis) Assay

Vasculogenesis-chips were fabricated using the polydimethylsiloxane soft lithography and were designed containing 5 parallel microchannels separated by hexagonal micro-posts spaced at 100 μm. Outer and central channels served as hydrogel compartments with widths of 1.5 mm, and fluid channels of 0.5-mm width were sandwiched between each hydrogel compartment. Each of the 5 microchannels were 8 mm long and terminated with port holes of 1-mm diameter for hydrogel channels and 5-mm diameter for fluid channels. Fibrin hydrogels were prepared by first dissolving bovine fibrinogen (Sigma-Aldrich) to 6 mg/mL in 1X PBS. Fibrinogen solutions were supplemented with 0.15 U/mL aprotinin (Sigma-Aldrich) and 0.2 mg/mL collagen I (Corning, Corning, NY, USA), as described previously.[22] Separately, normal human lung fibroblasts (NHLFs) (Lonza, Walkersville, MD, USA) and endothelial cells were lifted from their respective culturing flasks via trypsinization and resuspended in their media (Fibroblast growth media 2 for NHLFs [Lonza] and EGM2 for ECs) containing 5 U/mL bovine thrombin (Sigma-Aldrich) at concentrations of 6 million NHLFs/mL and 10 million ECs/mL. Fibrinogen and cell solutions were mixed 1:1, resulting in mixtures containing 3 mg/mL fibrinogen and 3 million NHLFs/mL or 5 million ECs/mL. Fibroblast pre-gelled solutions were injected into outer hydrogel compartments and EC pre-gelled solutions were injected into the central channel. Within minutes, the solutions gelled. Hydrogels were hydrated by injecting EGM2 into fluid channels. Then 50 μL EGM2 was added to each fluid reservoir and devices were incubated for 96 hours with daily media changes. After 96 hours, the chips were fixed and stained according to the method described above. Tiled Z-stacks images were assessed with Rapid Editable Analysis of Vessel Elements Routine (REAVER) software, which obtains microvascular network morphological characteristics.[23]

RNA Sequencing and Analysis

All cells were cultured in 6-well plates (n=4) and were detached using the method described above when cells reached 70% confluence. Once the cell pellets were collected, total mRNA was extracted using Monarch Total RNA Miniprep Kit (New England Biolabs) following the manufacturer's protocol. Before initiating RNA library preparation for sequencing, RNA quality was checked for all samples by measuring absorbance ratio 260/280 nm and only samples with ratios ≥2 were used. Samples were prepared using the TruSeq Standard Total RNA preparation kit (Illumina) and were then analyzed using NextSeq 500 platform (Illumina) at Molecular Genomics Workspace, Texas A&M University, College Station, TX. Postsequencing, raw paired end reads (1×75) were analyzed for quality using FastQC. Then we used HISAT2 to splice align the reads to latest ENSEMBL-release-102 human genome/transcriptome (GRCh38.p13). The number of sequenced reads for each replicate that were successfully mapped to the human genome are provided in the supplementary data (Table S1). To generate raw counts from alignment files (SAM), we used the Bioconductor package SUBREAD. Raw gene counts obtained from SUBREAD were then normalized using the "Relative Log Expression" or RLE normalization method used by the Bioconductor package, DESeq2.[24,25] For all genes, gene expression was defined when the gene counts across all replicates of each cell type was >10 (ie, genes with <10 count across all replicates were ignored). Differentially expressed genes were then evaluated for all groups using DESeq2 package in R. The cutoff to determine significant genes in all groups were false discovery rate adjusted *P* value (q-value)<0.05 and $-2 \leq \log_2$(fold change) ≥2.

Vessel-Chip Fabrication, Functionalization, and Endothelial Cell Culture

Microfluidic channels 200-μm wide, 75-μm high, and 2 cm long (hydraulic diameter: ≈110 μm) were fabricated using soft lithography of polydimethylsiloxane (Dow Corning). polydimethylsiloxane slabs containing features were cut out and inlet–outlet holes were punched using a 1.5-mm hole puncher (Ted Pella). The channels were then bonded to polydimethylsiloxane-coated glass slides using a 100-W plasma cleaner (Thierry Zepto, Diener Electronic). The devices were filled with 100 μg/mL solution of type-1 rat tail collagen and 50 μg/mL solution of fibronectin. The devices were incubated at 37 ˚C in a 5% CO_2 incubator for an hour after which the collagen–fibronectin solution was rinsed out with 1X PBS. Confluent flasks with respective cell types were trypsinized and cell pellets were collected after centrifugation. The cells were resuspended at a concentration of 10 million cells/mL and the cell suspensions were added to the microfluidic devices. The cells were allowed to attach to the basal matrix coating for an hour while being incubated at 37 ˚C in a 5% CO_2 incubator. The same process was repeated with a fresh cell suspension after an hour and the devices were incubated while being upside-down to allow cell attachment on all surfaces. An open slip-tip syringe was connected to the channels via a curved

dispensing tip (Qosina) that acted as a fluid reservoir. The cell-laden devices were connected to a syringe pump (Harvard Apparatus, PHD Ultra) through the outlet using a 20-in tubing (Qosina) and were perfused with respective cell growth media at 1 µL/min (shear stress: 0.81 dynes/cm^2; shear rate: 81 s^{-1}) for 24 hours. The flow rate was chosen to provide arteriolar shear conditions while optimizing growth media use.[26,27]

Growth Rate Measurement

Time–lapse images of live cells culturing on chip were taken using the Lux 2 microscope (CytoSMART) while placed in the incubator. Digital phase contrast images were acquired at a 10× magnification every 15 minutes until devices reached confluence. The cell coverage area within the devices was calculated by thresholding and converting the images to binary using ImageJ/Fiji. The total cell area was then summed over the entire field of view for all time–lapse images and the growth rates were reported as percent area coverage with respect to time.

Gap Measurement and Barrier Assessment

Confluent vessel-chips treated with or without tumor necrosis factor-α (TNF-α) were fixed using 4% paraformaldehyde for 15 minutes. The vessels were then permeabilized using 0.1% Triton in 2% BSA/DPBS for 10 minutes. The vessels were subsequently blocked with 2% BSA/DPBS for 30 minutes after which they were stained for VE cadherin, F-actin, and nuclei. The stained vessels were then imaged using a fluorescence microscope and images were analyzed in ImageJ/Fiji. Closed loops that did not contain nuclei were regarded as gaps.[16,28] The gap areas were summed over the entire field of view and reported as percentage area coverage.

Blood Perfusion and Image Analysis

All experiments were performed in accordance with the policies of the US Office of Human Research Protections and Texas A&M University Human Research Protection Program. The study was approved by the Texas A&M University Institutional Review Board (IRB ID: IRB2016-0762D) and subjects provided informed consent. Blood from healthy donors was collected in 3.2% sodium citrate tubes (BD Biosciences). To ensure consistent results and avoid abnormal coagulation activity, the blood samples were used within 4 hours of withdrawal. Five hundred microliters of blood sample was incubated with fluorescein isothiocyanate–conjugated anti-human CD41 antibody (10 µL/mL blood; Invitrogen) to label the platelets and fluorescently labeled fibrinogen (20 µg/mL blood, Invitrogen). Blood was perfused at a flow rate of 15 µL/min, which yielded a shear rate of 750 s^{-1}. To reinstate coagulation, a solution of 100 mmol/L $CaCl_2$ and 75 mmol/L $MgCl_2$ was mixed with blood in a 1:10 ratio before perfusion.[29] The devices were mounted on an automated microscope (Zeiss Axio Observer) and real-time fluorescence imaging was performed for a duration of 15 minutes. Once fluorescence time–lapse images were obtained, we used ImageJ to crop all images to a 700×200-µm size to exclude regions outside the channel from the analysis. The composite micrographs were then split into respective fibrin and platelet images for independent analysis. The subsequent analysis was performed for both fibrin and platelet micrographs independently. We used MATLAB to convert the respective images for all treatments to binary images with a threshold value of 0.2. The area coverage was then calculated as a ratio of total white pixels to the total number of pixels in the field of view for each treatment and reported as a percentage.

Statistical Analysis

All data are reported as mean±SD. All experiments were performed in triplicate (n=3) unless otherwise stated. Statistical comparisons were made either using 2-way ANOVA, repeated-measures 2-way ANOVA, Student *t* test, or Pearson correlation test in GraphPad Prism ver. 9. Differences were considered significant for $P<0.05$. Multiple testing correction was performed using the Tukey test in GraphPad Prism ver. 9.

RESULTS

Blood-Derived Endothelial Cells Exhibit Classic Endothelial Hallmarks

We initiated the study by assessing the typical endothelial characteristics of BOECs and identify extent of similarity with commercially available and typically used HUVECs and iECs. Endothelial cells are classically known to form monolayers in a “cobblestone” morphology under standard in vitro culture conditions.[30] We observed that blood-derived BOECs formed this classic cobblestone morphology along with the commercially obtained HUVECs and iECs in static conditions (Figure 2A). Furthermore, we found that the expression of VE-cadherin (regulator of endothelial tight junctions and permeability)[31]; vascular endothelial growth factor-A (growth factor that regulates angiogenesis and vasculogenesis); KDR (vascular endothelial growth factor receptor 2, a receptor–type tyrosine kinase known to influence cell migration[32]); platelet endothelial cell adhesion molecule-1 (CD31, endothelial cell adhesion molecule[33]) are conserved within BOECs and are comparable to HUVECs and iECs (Figure 2B), suggesting BOECs are mature endothelial cells with comparable typical expression profile to commercial cells. Next, we assessed the ability of these cells to migrate through the wound-healing assay

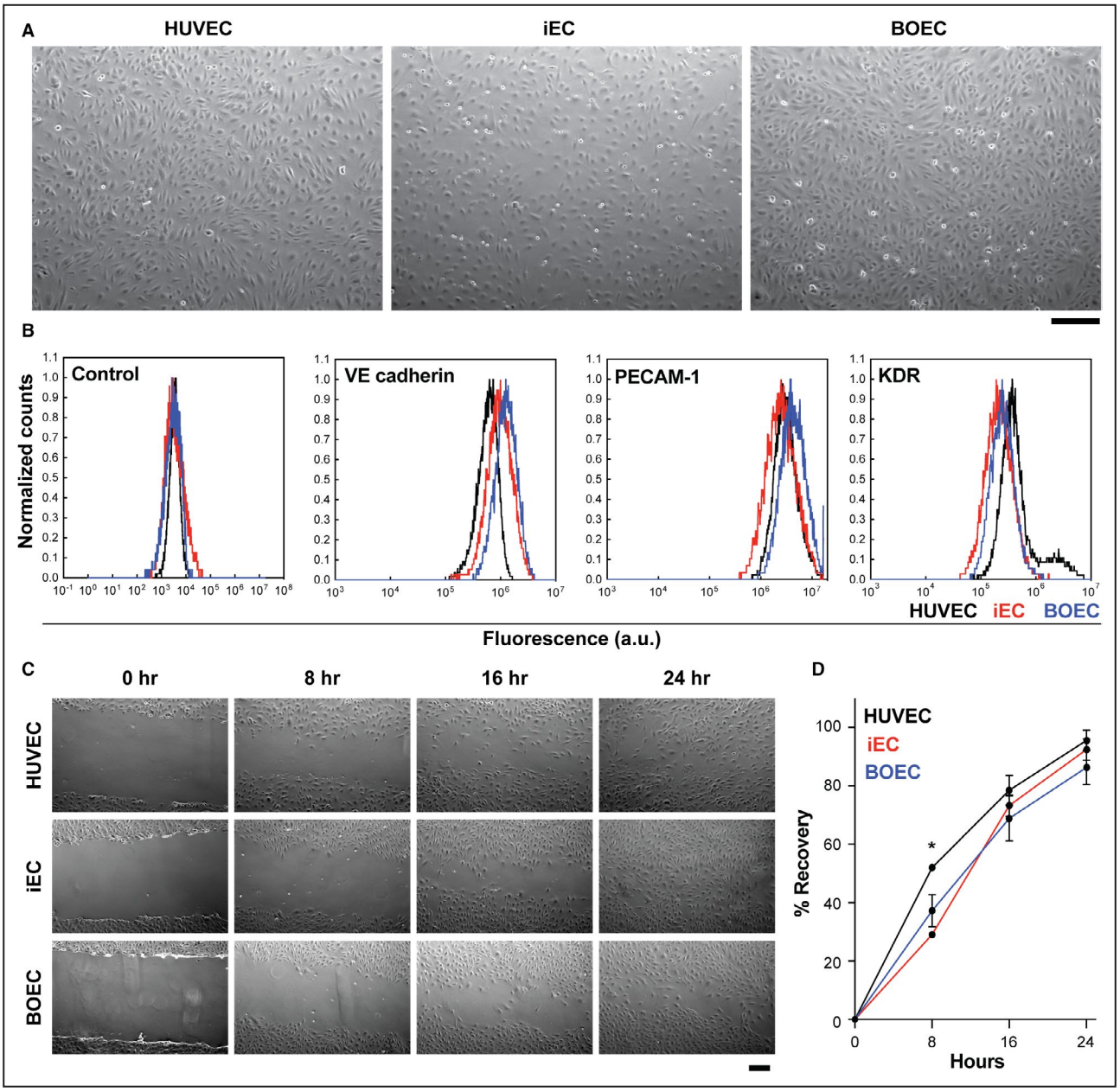

Figure 2. Assessment of the endothelial morphology, surface marker expression, and cell migration of endothelial cells. **A**, Phase contrast images of HUVEC iEC and BOEC exhibiting the classic endothelial "cobblestone" morphology (scale bar: 200 μm). **B**, Flow cytometry histograms of common endothelial markers VE-cadherin, KDR, and PECAM-1 for HUVECs (black), iECs (red), and BOECs (blue). **C**, Time–lapse images of scratch assay and subsequent endothelial cell migration for HUVECs, iECs, and BOECs. Images were taken every 8 hours and all 3 cell types exhibited nearly complete wound healing by 24 hours (scale bar: 100 μm). **D**, Quantification of wound healing rates for the HUVECs (black), iECs (red), and BOECs (blue). Data reported shows percent wound recovered with respect to wound area at t=0. *P<0.05 for iECs vs HUVECs at t=8 hours, calculated using repeated measures 2-way ANOVA. a.u. indicates arbitrary units; BOEC, blood outgrowth endothelial cells; HUVEC, human umbilical vein endothelial cells; iEC, induced pluripotent stem cell–derived endothelial cells; KDR, kinase domain receptor; PECAM-1, platelet endothelial cell adhesion molecule 1; and VE, vascular endothelial.

after a sustained injury to the endothelium.[34] Endothelial migration plays an important role in the formation of new blood vessels and repair of damaged tissue.[35] To assess how BOECs perform healing in vitro, we created a 1-mm scratch across confluent endothelial monolayers and performed subsequent time–lapse imaging of cell migration. Over the span of 24 hours, all cell types were able to migrate and heal the wound (Figure 2C). Quantifying the rate of cell migration revealed that HUVECs, iECs, and BOECs had similar growth/recovery rates over the span of 24 hours (Figure 2D). These results suggest that BOECs have a similar growth and migration

response to an injury compared with HUVECs and iECs, further strengthening the hypothesis that they are a useful cell model for in vitro research.

Assessment of Vasculogenic Potential of Blood-Derived Endothelial Cells

Since organ-on-chips are regularly used to form vascular networks, we also set out to investigate the vasculogenic abilities of BOECs as compared with traditionally used cells using the common vasculogenesis-chip model where compartmentalized hydrogels encapsulate vascular and stromal cell types separated by narrow fluidic channels.[22,36] Vasculogenesis-chips were either cultured in monoculture (EC only) or cocultured with fibroblasts (EC + NHLF) to determine both the de novo vascularization potential of unstimulated endothelial cells

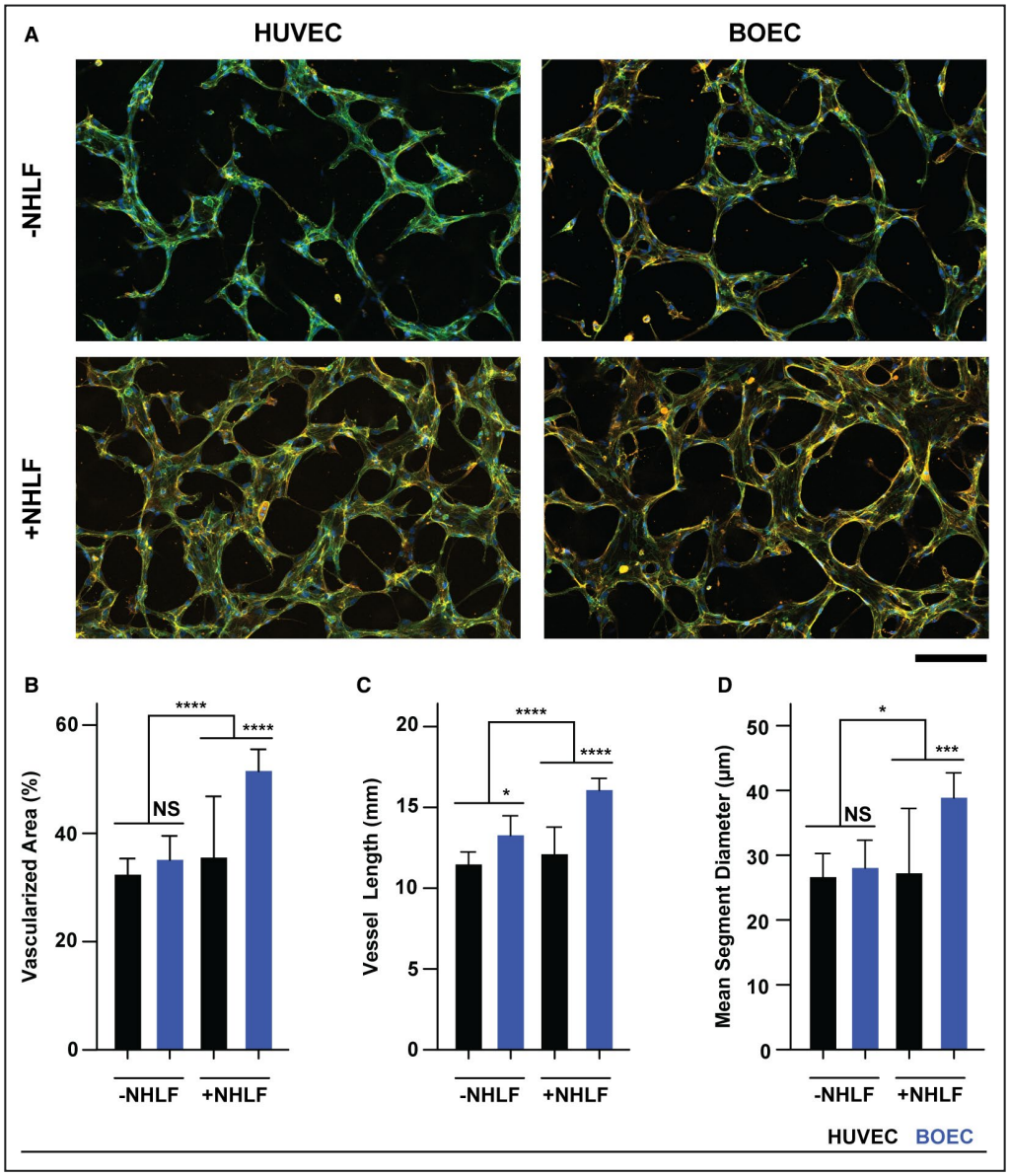

Figure 3. Assessment of vasculogenic potential of endothelial cells with and without stimulation with fibroblasts.

A, Fluorescence micrographs of blood vessel formation or vasculogenesis after 96 hours of culture with and without fibroblasts. (green: CD31, yellow: F-actin, blue: nuclei; scale bar: 100 µm). **B** through **D**, Quantified vessel formation metrics such as vascularized area (**B**), vessel length (**C**), and mean segment diameter (**D**). **P*<0.05, ****P*<0.0005, *****P*<0.0001; (**B** through **D**): (HUVEC, black) and blood outgrowth endothelial cells (BOEC, blue). *P* values calculated using 2-way ANOVA. BOEC indicates blood outgrowth endothelial cells; HUVEC, human umbilical vein endothelial cells; NHLF, normal human lung fibroblast; and NS, not significant.

as well as each cell type's response to pro-vascular stromal fibroblasts (NHLFs). After a 96-hour culturing period with daily media changes, both HUVEC and BOEC monoculture chips formed microvascular networks (Figure 3A). When iECs were cultured in the vasculogenesis-chip and assessed for vessel formation, we observed that they were unable to form confluent networks in the same time (Figure S1), possibly because of the use of standard culture media across all cell types and not adding additional supplements.[37–39] Since BOECs do not require expensive reagents and growth factors as well as sophisticated cell differentiation protocols requiring extensive training, BOECs also exhibited conserved morphological properties in cultures until passages 9–10 (Figure S2A) compared with iECs that could only maintain their morphology until passage 5 (Figure S2B). Their increased survival in vitro makes BOECs suitable for long-term clinical studies because they can be cryopreserved in a timely manner and cultured again.

Addition of fibroblasts provided an additional growth stimulus to the endothelial cells, which improved the overall quality of the newly formed vascular networks. Co-culture conditions exhibited increased vascularized area, vessel length, and the mean vessel diameter of networks compared with monoculture conditions (Figure 3B through 3D). Interestingly, BOECs performed better in both monoculture and co-culture platforms, demonstrating their sensitivity to growth factors and cell signaling from parenchymal region. Since vasculogenesis is mostly seen during embryonic development and arises from islands of endothelial progenitors spontaneously forming tubular vasculature, BOECs may be very useful for de novo vascularization within organ-on-chips.[40]

Evaluation of Transcriptomic Profiles of Different Endothelial Cells Through RNA Sequencing

After standard endothelial characterization, we analyzed the transcriptomic behavior of BOECs and evaluated their transcript level differences through whole genome RNA sequencing of endothelial cells. RNA from respective cells was isolated and processed for RNA sequencing after quality assessment (Figure 4A). Upon sequencing, we generated gene counts for all the genes expressed by each cell type. We observed that HUVECs expressed ≈16 300 genes, while iECs expressed ≈16 700 genes and BOECs expressed ≈15 550 genes. Out of these, ≈15 250 genes were common between HUVECs and iECs, ≈15 150 genes were common among HUVECs and BOECs, ≈14 850 genes were common between iECs and BOECs, and finally, ≈14 600 genes were common among all the cells (Figure 4B). We then investigated the expression of genes belonging to key endothelial activation and regulation pathways according to the Kyoto Encyclopedia of Genes and Genomes (KEGG) pathway clustering. Genes belonging to Cell adhesion molecules (CAMs; KEGG:04514), extracellular matrix (ECM)–receptor interaction (KEGG:04512), Focal adhesion (KEGG:04510), Complement and coagulation cascades (KEGG:04610), Platelet activation (KEGG:04611), Cytokine–cytokine receptor interaction (KEGG:04060), TNF signaling (KEGG:04668), and Fluid shear stress and atherosclerosis (KEGG:05418) pathways were analyzed (Figure 4C). Interestingly, we observed that iECs had a nearly contrasting expression profile compared with HUVECs, with ≈70% genes being expressed opposingly. This opposing behavior further suggests that iECs are transcriptomically different from their primary endothelial cell counterparts. This was further confirmed by generating pairwise gene correlation plots of iECs and BOECs with respect to HUVECs (Figure 4D and 4E). Compared with BOECs, iECs had a poorer correlation with the HUVEC gene expression profile. On the other hand, BOEC gene expression was closer to that of HUVECs because more genes were clustered along the $y=x$ line (slope=45°).

The transcriptomic similarity of iECs and BOECs with respect to HUVECs was further confirmed by calculating the pairwise Pearson correlation coefficient (r) between cell types. As expected, BOECs had a higher

Figure 4. Qualitative assessment of differential gene expression of iECs and BOECs compared with primary HUVECs.
A, Schematic of the RNA sequencing process followed in the study. mRNA from HUVECs, iECs, and BOEC was extracted and processed for sequencing post quality assessment. **B**, Venn diagram depicting the sets of common and unique genes expressed by each endothelial cell type. **C**, Heatmap depicting row-scaled z-score of genes belonging to various endothelial activation pathways predicted by the KEGG database: (CAMs; KEGG:04514), ECM–receptor interaction (KEGG:04512), Focal adhesion (KEGG:04510), Complement and coagulation cascades (KEGG:04610), Platelet activation (KEGG:04611), and Cytokine–cytokine receptor interaction (KEGG:04060), TNF signaling (KEGG:04668), Fluid shear stress, and atherosclerosis (KEGG:05418) pathways. iECs had a nearly opposite expression profile compared with HUVECs with ≈70% genes being expressed contrastingly. On the other hand, BOECs had an expression profile that was closer to HUVECs with ≈40% genes being contrastingly expressed. **D**, Pairwise correlation of gene expression between iECs (y-axis) and HUVECs (x-axis). Values plotted are $\log_2$(count) values for each gene with an R^2 value of 0.78. **E**, Pairwise correlation of gene expression between BOECs (y-axis) and HUVECs (x-axis). Values plotted are $\log_2$(count) values for each gene with an R^2 value of 0.87. **F**, Pearson correlation coefficient, r, calculated for pairwise gene expression between iEC-HUVEC and BOEC–HUVEC pairs. BOECs demonstrated a higher correlation with HUVECs compared with iECs. BOECs indicates blood outgrowth endothelial cells; CAMs, cell adhesion molecules; ECM, extracellular matrix; HUVECs, human umbilical vein endothelial cells; iECs, induced pluripotent stem cell–derived endothelial cells; KEGG, Kyoto Encyclopedia of Genes and Genomes; and TNF, tumor necrosis factor.

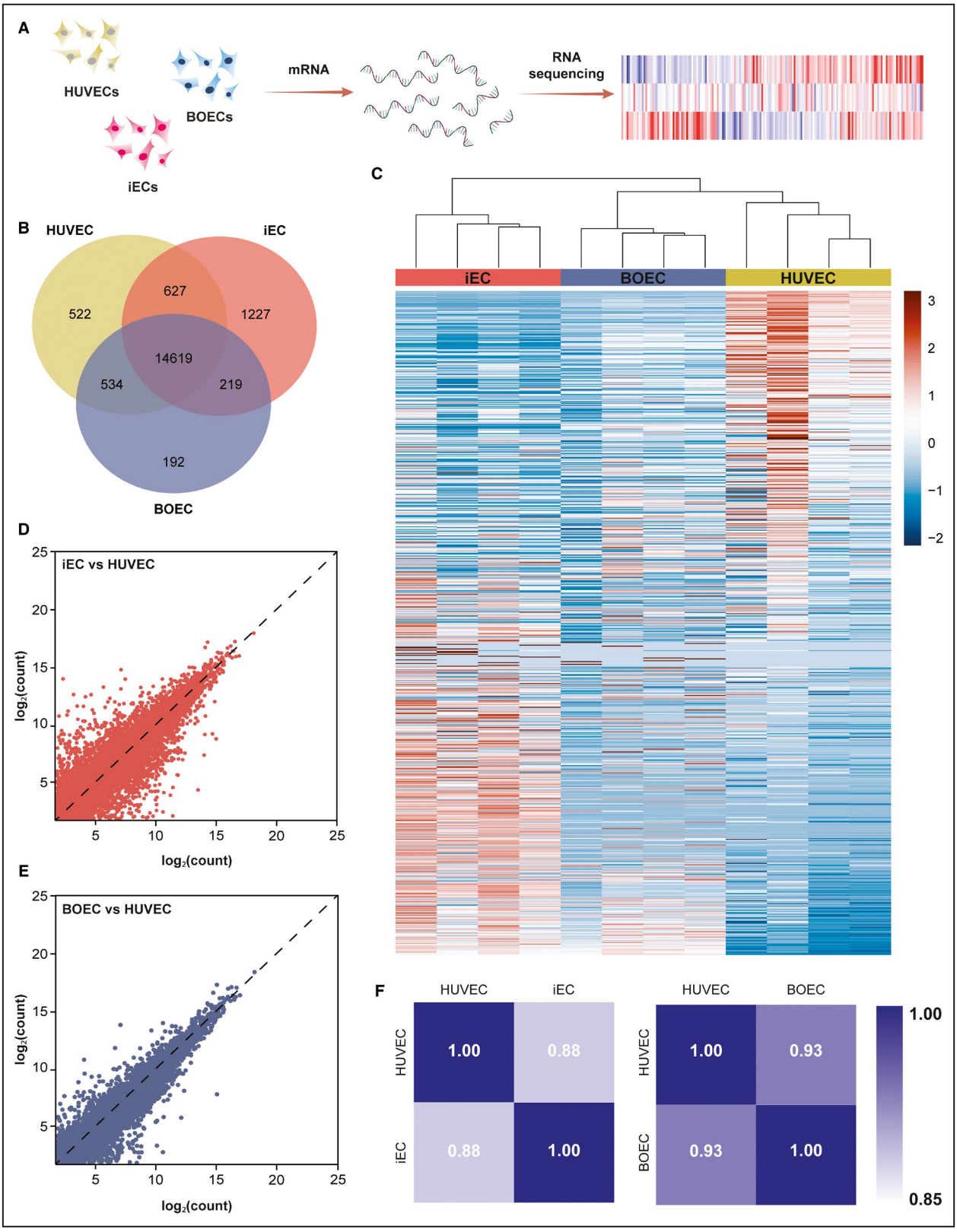

correlation with HUVECs than iECs, suggesting that BOEC transcriptomic profile might indeed be closer to that of HUVECs.

We then performed differential gene expression analysis of iECs and BOECs against HUVECs, which was our primary control endothelial cell type,

to statistically validate the differential gene expression. When compared with HUVECs, iECs expressed ≈3600 genes, out of which ≈1950 were upregulated and ≈1700 were downregulated. On the other hand, the number of differentially expressed genes belonging to BOECs was ≈1400, with ≈470 genes upregulated and ≈940 genes downregulated (Figure S2A). This difference in number of differentially expressed genes between the 2 cell types suggests that the transcriptomic behavior of iECs might be significantly different from HUVECs, which have been routinely used in research as an endothelial cell model. In contrast, BOECs have a significantly lower number of differentially expressed genes compared with iECs, suggesting that they are closer to HUVECs with respect to their transcriptomic behavior. The differences in the extent of gene expression between iECs and BOECs could further be visualized through volcano plots (Figure S2B and S2C). Despite differences in the number of genes expressed between the 2 cell types, iECs exhibited a much more diverse expression profile with greater magnitude of gene upregulation/downregulation (fold change), which further suggests that transcriptomic profiles of iECs are significantly different from HUVECs, while BOECs exhibit gene expression that is closer to HUVECs. This difference might be dependent on the isolation protocol used by the commercial source or it could also depend on the lineage of the precursor cells used to generate iPSCs.[41] Some heterogeneity after differentiation could also exist and further contribute to variable gene expression between HUVECs and iECs.[42] Contrastingly, BOECs exhibited an expression profile that was closer to HUVECs, with only ≈40% of genes exhibiting opposing expression (Figure 4E). The difference in the expression of these genes could be attributed to the hematopoietic lineage of the endothelial progenitors from which BOECs form. Therefore, the transcriptomic closeness of BOECs to HUVEC relative to commercially obtained iECs strengthens the findings that BOECs are excellent primary cells for modeling studies.

Response of Endothelial Cells to Fluid Shear in Vessel-Chips

After RNA-seq, we leveraged our vessel-chip designs to study the differential effects of fluid flow on endothelial cells.[15,16] We cultured HUVECs, iECs, and BOECs in 200-μm wide and 75-μm high vessel-chips (Figure 5A and 5B) under constant growth media perfusion (1 μL/min, 0.81 dynes/cm^2). We then evaluated the rate of growth of these cells because of shear (Figure 5C). Interestingly, while BOECs had similar growth kinetics compared with HUVECs and covered the surfaces within 24 hours, iECs exhibited a slower growth rate and were not able to become confluent within 24 hours, possibly because of the transcriptomic differences that we observed earlier. In fact, even when iECs were uniformly distributed in the vessel-chip after initial seeding into matrix-coated microchannels (Figure S3A), the cells were unable to become confluent within the first 24 hours (Figure S3B). After culturing cells for an additional 24 hours (total 48 hours) compared with other endothelial cell types, iEC vessel-chips still exhibited large gaps in the endothelium (Figure S3C). Since endothelial cells align along the directions of fluid flow,[43] we also found that all 3 cell types showed alignment along the flow direction after a 24- hour perfusion culture (Figure 5D), which we also confirmed quantitatively (Figure 5E). These morphological characteristics were further confirmed by noticing that cell area increased (Figure 5F), and circularity decreased over the 24-hour culture period on-chip (Figure 5G). These results collectively suggest that BOECs grow relatively faster than iECs within organ-chips and they are actively shear sensitive, possessing similar responses to shear activation in vitro against the commercially available cells.

Assessment of Endothelial Barrier Integrity After Cytokine Stimulation Through Vessel-Chips

Next, we set out to assess the barrier function of endothelial cells but we were compelled to omit iECs in these vessel-chip functional studies because they failed to form confluent endothelial monolayers using standard protocols provided by the manufacturer, or typically used in the literature. To assess the barrier function of BOECs with respect to HUVECs, we compared the presence of small gaps in the lumen of respective vessel-chips through fluorescence microscopy (Figure 6A). Endothelial cells exhibit impairment of their barrier capabilities after interacting with cytokines, and vascular leakage is an important hallmark of inflammation.[44,45] In agreement with this behavior, BOECs and HUVECs both showed increase in microscopic gaps in the lumen after a 5 ng/mL TNF-α stimulation for 6 hours (Figure 6A and 6B).

Evaluation of Cytokine-Stimulated Thromboinflammation Through Vessel-Chips

To study the thromboinflammatory consequences of cytokine stimulation and evaluate differences in the extent of thrombi formation in the respective vessel-chips, we stimulated confluent vessel-chips with and without 5 ng/mL TNF-α. After a 6-hour incubation with TNF-α, we perfused recalcified whole blood at arteriolar conditions and performed time–lapse fluorescence microscopy to observe the real-time platelet adhesion and fibrin deposition for the respective vessel-chips.

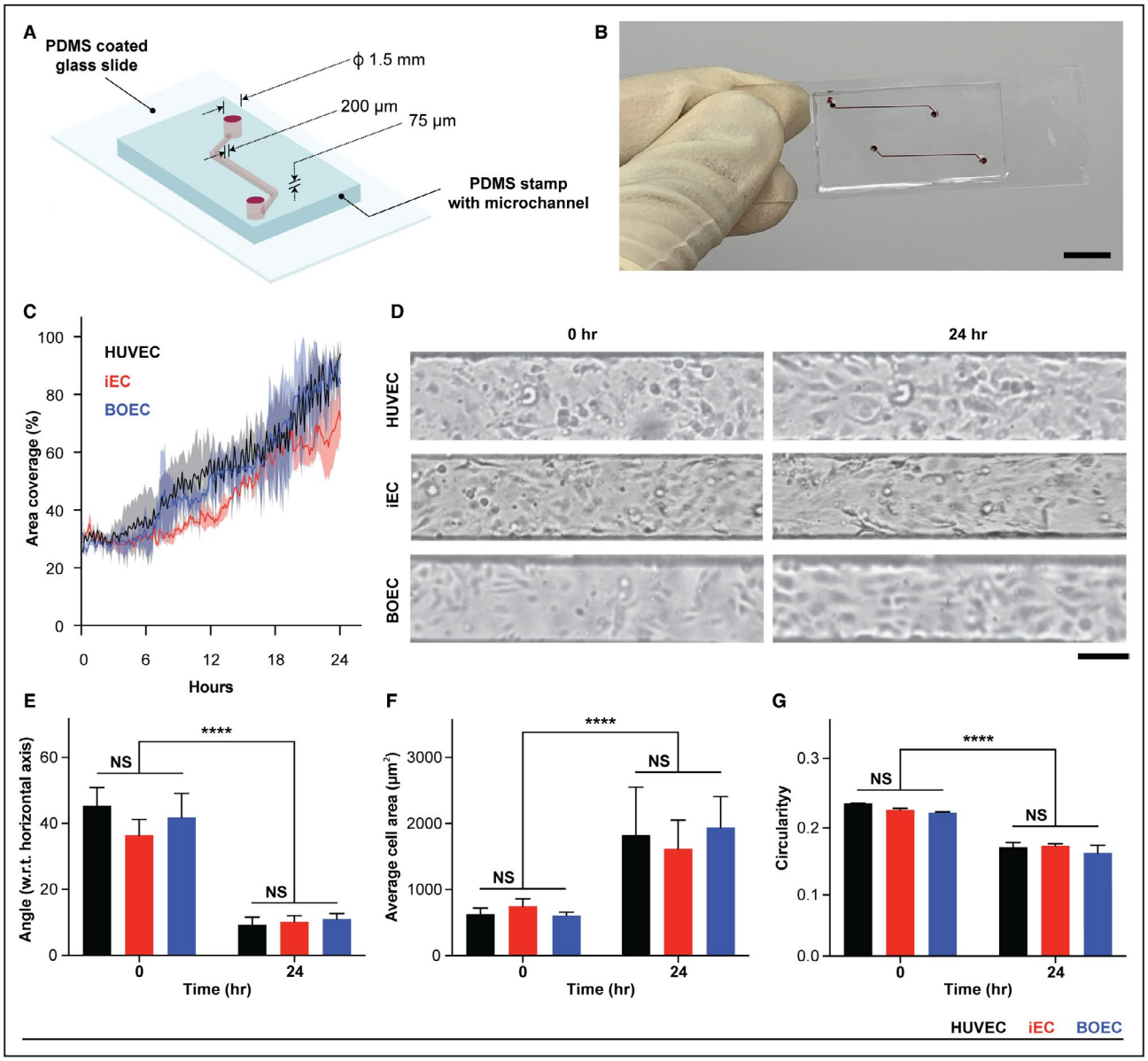

Figure 5. Assessment of growth kinetics and response to shear through vessel-chip.
A, Schematic of the microfluidic channels employed in the study. The channels are 200-µm wide and 75-µm high. The inlet and outlet holes were 1.5-mm wide. **B**, Each device contained 2 independent microchannels for performing multiple experiments (scale bar: 1 mm). **C**, Graph showing the growth rates of (HUVEC, black), (iEC, red), and (BOEC, blue) with time when cultured in microfluidic chips under constant shear. Solid lines represent mean and shaded areas represent error (SD). **D**, Time–lapse images of cell alignment under laminar shear at t=0 and t=24 hours showing that all 3 cells respond to shear and align along the flow direction (scale bar: 100 µm). **E**, Quantification of directionality of aligned endothelial cells with respect to flow direction (horizontal from left to right). **F**, Quantification of average cell area before and after perfusion culture for endothelial cells. **G**, Quantified average circularity of endothelial cells after perfusion culture. ****P<0.0001; legend (**C** through **E**): HUVECs (black), iECs (red) and BOECs (blue). P values calculated using 2-way ANOVA. BOEC indicates blood outgrowth endothelial cells; HUVEC, human umbilical vein endothelial cells; iEC, induced pluripotent stem cell–derived endothelial cells; NS, not significant; PDMS, polydimethylsiloxane; and w.r.t., with respect to.

We observed that both HUVECs and BOECs exhibited increased platelet–endothelial interactions and had significantly increased fibrin formation (Figure 6C). In addition, the extent of platelet adhesion and fibrin formation was similar between HUVECs and BOECs (Figure 6D and 6E). Interestingly, both vessel-chips exhibited the formation of "comet"-shaped thrombi under physiological blood flow that has been observed in vivo, as well as some in vitro studies using HUVECs[9,46] (Figure 6F). These results suggest that BOECs have a similar thromboinflammatory response to cytokine activation compared with HUVECs and hence can be a suitable alternative for developing vascular models of thrombosis observed in different disease modalities.

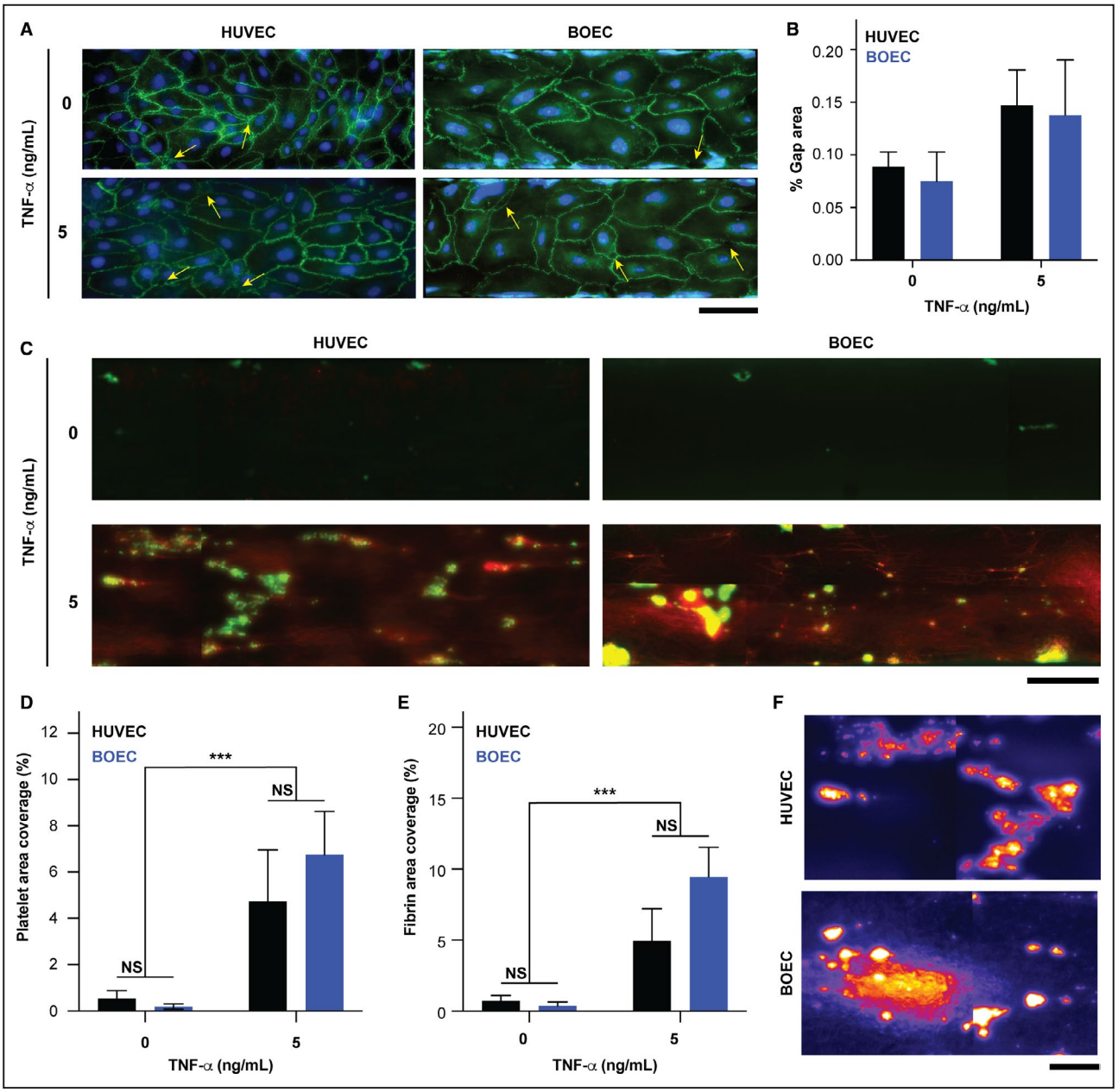

Figure 6. Assessment of endothelial barrier function and thromboinflammation of endothelial cells.
A, Fluorescence micrographs of HUVEC and BOEC depicting gaps (arrows) before and after TNF-α stimulation (green: VE-cadherin, blue: nuclei; scale bar: 100 μm). **B**, Quantification of gap area of endothelial cells with respect to TNF-α stimulation. **C**, Fluorescence micrographs of platelet adhesion (green) and fibrin formation (red) over unstimulated and stimulated vessel-chips. HUVECs and BOECs attain a prothrombotic phenotype after TNF-α treatment and cause thrombosis and fibrin coagulation (scale bar: 100 μm). **D** and **E**, Quantified platelet area coverage (**B**) and fibrin content (**C**) in respective vessel-chips. **F**, Both endothelial cells form "comet"-shaped thrombi under constant blood flow (scale bar: 50 μm). ***P<0.0005; legend (**B** through **C**): HUVECs (black) and BOECs (blue). P values calculated using 2-way ANOVA. BOEC indicates blood outgrowth endothelial cells; HUVEC, human umbilical vein endothelial cells; NS, not significant; TNF-α, tumor necrosis factor-α; and VE, Vascular Endothelial.

DISCUSSION

The aim of this study is to help researchers identify potential autologous endothelial cells for developing physiologically relevant vascular disease modeling platforms such as vessel-chip that can ultimately aid in discerning the milieu of signaling and pathophysiological events contributing to the patient-to-patient variation observed clinically. Our results here collectively suggest that BOECs are an excellent potential alternative to the current endothelial cell sources. This is confirmed by analyzing their surface marker expression, morphology, growth kinetics, and responses to shear stress and cytokine exposure. Since iPSC-derived ECs are being

increasingly used in preclinical organ-chip research as a potential autologous cell source obtained from patients, we analyzed them as another autologous cell model for comparing with BOECs, which might also be potential patient-specific cell sources. Endothelial progenitors such as BOECs have been utilized in previous cardiovascular studies to study the ex vivo biology of diseased ECs from chronic obstructive pulmonary disease,[47] pulmonary hypertension,[48] and von Willebrand disease[49,50] among many others. Our own previous work with patient-derived BOECs suggested that they are able to carry the disease phenotype when cultured in vitro in microphysiological vessel-chips.[16] In addition to being disease specific, autologous BOECs were also effective in recapitulating some patient-specific hallmarks of vascular complications in vitro.[15]

However, using BOECs in preclinical research requires some attention. Although patient-derived BOECs are proliferative, several studies have reported variability in obtaining colonies postisolation from whole blood, with success rates varying from zero for certain individuals up to ≈75% in some cases.[17,51] Additionally, several groups have reported that endothelial progenitors decrease in patients with cardiovascular disease compared with healthy individuals.[51,52] To accommodate these limitations, alternative and sensitive isolation techniques might need to be used and amount of whole blood used to generate colonies might need to be optimized. Despite these nuances, the disease- and patient-phenotype expressing ability of BOECs warrant further characterization and phenotyping studies in the context of large patient cohorts.

Overall, our results bolster the use of endothelial progenitors such as BOECs as an EC model that can be used in clinical research for developing more robust and humanized disease models that circumvent the need for using primary cells such as HUVECs. This will ultimately enable next-generation organ-on-chip biotechnology to make a positive impact on medicine and health care.

ARTICLE INFORMATION

Received June 7, 2021; accepted October 6, 2021.

Affiliations

Department of Biomedical Engineering, College of Engineering, Texas A&M University, College Station, TX (T.M., J.J.T., A.J.); Department of Medical Physiology, College of Medicine, Texas A&M Health Science Center, Bryan, TX (A.J.); and Department of Cardiovascular Sciences, Houston Methodist Research Institute, Houston, TX (A.J.).

Acknowledgments

The authors would like to thank Dr Andrew Hillhouse at the Molecular Genomics Workspace, Texas A&M Institute for Genomic Sciences and Society (TIGGS) for analyzing the extracted RNA for quality and performing RNA sequencing. We also thank Ms. Jo Ann Culpepper at A.P. Beutel Health Center, Texas A&M University for managing the phlebotomy of healthy donors and providing blood samples. The authors would also like to thank Mr Kanwar Abhay Singh in the Department of Biomedical Engineering at Texas A&M University for assisting with flow cytometry.

Author contributions: T.M. and A.J. designed the experiments and analyzed data. T.M., J.T., and A.J. wrote the manuscript. T.M. fabricated the devices, isolated blood outgrowth endothelial cells, cultured the cells, and performed the experiments. J.T. performed blood vessel formation assay.

Sources of Funding

This study was made possible by the National Institutes of Biomedical Imaging and Bioengineering of NIH under Award Number R21EB025945 (AJ), National Science Foundation Career Award 1944322 (AJ), the Texas A&M Triads for Transformation (T3) program by President's Excellence Fund (AJ), Texas A&M Engineering Experimentation Station (TEES), and Texas A&M University.

Disclosures

None.

Supplementary Material

Table S1
Figures S1–S3

REFERENCES

1. Roth GA, Mensah GA, Johnson CO, Addolorato G, Ammirati E, Baddour LM, Barengo NC, Beaton AZ, Benjamin EJ, Benziger CP, et al. Global burden of cardiovascular diseases and risk factors, 1990–2019: update from the GBD 2019 study. *J Am Coll Cardiol*. 2020;76:2982–3021. doi: 10.1016/j.jacc.2020.11.010
2. Yusuf S, Reddy S, Ounpuu S, Anand S. Global burden of cardiovascular diseases: part i: general considerations, the epidemiologic transition, risk factors, and impact of urbanization. *Circulation*. 2001;104:2746–2753. doi: 10.1161/hc4601.099487
3. McLaughlin T, Abbasi F, Lamendola C, Reaven G. Heterogeneity in the prevalence of risk factors for cardiovascular disease and type 2 diabetes mellitus in obese individuals: effect of differences in insulin sensitivity. *Arch Intern Med*. 2007;167:642–648. doi: 10.1001/archinte.167.7.642
4. Aldossri M, Farmer J, Saarela O, Rosella L, Quiñonez C. Oral health and cardiovascular disease: mapping clinical heterogeneity and methodological gaps. *JDR Clin Trans Res*. 2020;6:390–401.
5. Azizgolshani H, Coppeta JR, Vedula EM, Marr EE, Cain BP, Luu RJ, Lech MP, Kann SH, Mulhern TJ, Tandon V, et al. High-throughput organ-on-chip platform with integrated programmable fluid flow and real-time sensing for complex tissue models in drug development workflows. *Lab Chip*. 2021;21:1454–1474. doi: 10.1039/D1LC00067E
6. Low LA, Tagle DA. Tissue chips – innovative tools for drug development and disease modeling. *Lab Chip*. 2017;17:3026–3036. doi: 10.1039/C7LC00462A
7. Ronaldson-Bouchard K, Vunjak-Novakovic G. Organs-on-a-chip: a fast track for engineered human tissues in drug development. *Cell Stem Cell*. 2018;22:310–324. doi: 10.1016/j.stem.2018.02.011
8. Barrile R, van der Meer AD, Park H, Fraser JP, Simic D, Teng F, Conegliano D, Nguyen J, Jain A, Zhou M, et al. Organ-on-chip recapitulates thrombosis induced by an anti-cd154 monoclonal antibody: translational potential of advanced microengineered systems. *Clin Pharmacol Ther*. 2018;104:1240–1248. doi: 10.1002/cpt.1054
9. Jain A, van der Meer AD, Papa AL, Barrile R, Lai A, Schlechter BL, Otieno MA, Louden CS, Hamilton GA, Michelson AD, et al. Assessment of whole blood thrombosis in a microfluidic device lined by fixed human endothelium. *Biomed Microdevices*. 2016;18:73. doi: 10.1007/s10544-016-0095-6
10. Tsai M, Kita A, Leach J, Rounsevell R, Huang JN, Moake J, Ware RE, Fletcher DA, Lam WA. In vitro modeling of the microvascular occlusion and thrombosis that occur in hematologic diseases using microfluidic technology. *J Clin Invest*. 2012;122:408–418. doi: 10.1172/JCI58753
11. Cochrane A, Albers HJ, Passier R, Mummery CL, van den Berg A, Orlova VV, van der Meer AD. Advanced in vitro models of vascular biology: human induced pluripotent stem cells and organ-on-chip technology. *Adv Drug Deliv Rev*. 2019;140:68–77. doi: 10.1016/j.addr.2018.06.007
12. Sances S, Ho R, Vatine G, West D, Laperle A, Meyer A, Godoy M, Kay PS, Mandefro B, Hatata S, et al. Human iPSC-derived endothelial cells and microengineered organ-chip enhance neuronal development. *Stem Cell Reports*. 2018;10:1222–1236. doi: 10.1016/j.stemcr.2018.02.012

13. Doss MX, Sachinidis A. Current challenges of iPSC-based disease modeling and therapeutic implications. *Cells*. 2019;8:403.
14. Ohnuki M, Takahashi K. Present and future challenges of induced pluripotent stem cells. *Philos Trans R Soc Lond B Biol Sci*. 2015;370:20140367. doi: 10.1098/rstb.2014.0367
15. Mathur T, Flanagan JM, Jain A. Tripartite collaboration of blood-derived endothelial cells, next generation RNA sequencing and bioengineered vessel-chip may distinguish vasculopathy and thrombosis amongst sickle cell disease patients. *Bioeng Transl Med*. 2021;6:e10211. doi: 10.1002/btm2.10211
16. Mathur T, Singh KA, R. Pandian NK, Tsai SH, Hein TW, Gaharwar AK, Flanagan JM, Jain A. Organ-on-chips made of blood: endothelial progenitor cells from blood reconstitute vascular thromboinflammation in vessel-chips. *Lab Chip*. 2019;19:2500–2511. doi: 10.1039/C9LC00469F
17. Martin-Ramirez J, Hofman M, van den Biggelaar M, Hebbel RP, Voorberg J. Establishment of outgrowth endothelial cells from peripheral blood. *Nat Protoc*. 2012;7:1709–1715. doi: 10.1038/nprot.2012.093
18. Cheung AL. Isolation and culture of human umbilical vein endothelial cells (HUVEC). *Curr Protoc Microbiol*. 2007; Appendix 4:Appendix 4B.
19. Bang JS, Choi NY, Lee M, Ko K, Lee HJ, Park YS, Jeong D, Chung HM, Ko K. Optimization of episomal reprogramming for generation of human induced pluripotent stem cells from fibroblasts. *Anim Cells Syst (Seoul)*. 2018;22:132–139. doi: 10.1080/19768354.2018.1451367
20. Crampton SP, Davis J, Hughes CC. Isolation of human umbilical vein endothelial cells (HUVEC). *J Vis Exp*. 2007;183:183.
21. Cheng Z, Verma SK, Losordo DW, Kishore R. Reprogrammed human endothelial cells: a novel cell source for regenerative vascular medicine. *Circ Res*. 2017;120:756–758. doi: 10.1161/CIRCRESAHA.117.310573
22. Kim S, Lee H, Chung M, Jeon NL. Engineering of functional, perfusable 3D microvascular networks on a chip. *Lab Chip*. 2013;13:1489–1500. doi: 10.1039/c3lc41320a
23. Corliss BA, Doty RW, Mathews C, Yates PA, Zhang T, Peirce SM. Reaver: a program for improved analysis of high-resolution vascular network images. *Microcirculation*. 2020;27:e12618. doi: 10.1111/micc.12618
24. Abbas-Aghababazadeh F, Li Q, Fridley BL. Comparison of normalization approaches for gene expression studies completed with high-throughput sequencing. *PLoS One*. 2018;13:e0206312. doi: 10.1371/journal.pone.0206312
25. Anders S, Huber W. Differential expression analysis for sequence count data. *Genome Biol*. 2010;11:R106. doi: 10.1186/gb-2010-11-10-r106
26. Rajeeva Pandian NK, Walther BK, Suresh R, Cooke JP, Jain A. Microengineered human vein-chip recreates venous valve architecture and its contribution to thrombosis. *Small*. 2020;16:2003401. doi: 10.1002/smll.202003401
27. Perktold K, Resch M, Peter RO. Three-dimensional numerical analysis of pulsatile flow and wall shear stress in the carotid artery bifurcation. *J Biomech*. 1991;24:409–420. doi: 10.1016/0021-9290(91)90029-M
28. Aragon-Sanabria V, Pohler SE, Eswar VJ, Bierowski M, Gomez EW, Dong C. VE-Cadherin disassembly and cell contractility in the endothelium are necessary for barrier disruption induced by tumor cells. *Sci Rep*. 2017;7:45835. doi: 10.1038/srep45835
29. Jain A, Graveline A, Waterhouse A, Vernet A, Flaumenhaft R, Ingber DE. A shear gradient-activated microfluidic device for automated monitoring of whole blood haemostasis and platelet function. *Nat Commun*. 2016;7:10176. doi: 10.1038/ncomms10176
30. Tsuji-Tamura K, Ogawa M. Morphology regulation in vascular endothelial cells. *Inflamm Regen*. 2018;38:25. doi: 10.1186/s41232-018-0083-8
31. Vestweber D. Ve-cadherin: the major endothelial adhesion molecule controlling cellular junctions and blood vessel formation. *Arterioscler Thromb Vasc Biol*. 2008;28:223–232. doi: 10.1161/ATVBAHA.107.158014
32. Kanno S, Oda N, Abe M, Terai Y, Ito M, Shitara K, Tabayashi K, Shibuya M, Sato Y. Roles of two VEGF receptors, Flt-1 and KDR, in the signal transduction of VEGF effects in human vascular endothelial cells. *Oncogene*. 2000;19:2138–2146. doi: 10.1038/sj.onc.1203533
33. Woodfin A, Voisin MB, Nourshargh S. Pecam-1: a multi-functional molecule in inflammation and vascular biology. *Arterioscler Thromb Vasc Biol*. 2007;27:2514–2523. doi: 10.1161/ATVBAHA.107.151456
34. Jonkman JE, Cathcart JA, Xu F, Bartolini ME, Amon JE, Stevens KM, Colarusso P. An introduction to the wound healing assay using live-cell microscopy. *Cell Adh Migr*. 2014;8:440–451. doi: 10.4161/cam.36224
35. van der Meer AD, Vermeul K, Poot AA, Feijen J, Vermes I. A microfluidic wound-healing assay for quantifying endothelial cell migration. *Am J Physiol Heart Circ Physiol*. 2010;298:H719–725. doi: 10.1152/ajpheart.00933.2009
36. Osaki T, Sivathanu V, Kamm RD. Engineered 3D vascular and neuronal networks in a microfluidic platform. *Sci Rep*. 2018;8:5168. doi: 10.1038/s41598-018-23512-1
37. Campisi M, Shin Y, Osaki T, Hajal C, Chiono V, Kamm RD. 3D self-organized microvascular model of the human blood-brain barrier with endothelial cells, pericytes and astrocytes. *Biomaterials*. 2018;180:117–129. doi: 10.1016/j.biomaterials.2018.07.014
38. Lee SWL, Campisi M, Osaki T, Possenti L, Mattu C, Adriani G, Kamm RD, Chiono V. Modeling nanocarrier transport across a 3D in vitro human blood-brain-barrier microvasculature. *Adv Healthc Mater*. 2020;9:e1901486. doi: 10.1002/adhm.201901486
39. Belair DG, Whisler JA, Valdez J, Velazquez J, Molenda JA, Vickerman V, Lewis R, Daigh C, Hansen TD, Mann DA, et al. Human vascular tissue models formed from human induced pluripotent stem cell derived endothelial cells. *Stem Cell Rev Rep*. 2015;11:511–525. doi: 10.1007/s12015-014-9549-5
40. Patel-Hett S, D'Amore PA. Signal transduction in vasculogenesis and developmental angiogenesis. *Int J Dev Biol*. 2011;55:353–363. doi: 10.1387/ijdb.103213sp
41. Wiseman E, Zamuner A, Tang Z, Rogers J, Munir S, Di Silvio L, Danovi D, Veschini L. Integrated multiparametric high-content profiling of endothelial cells. *SLAS Discov*. 2019;24:264–273. doi: 10.1177/2472555218820848
42. Paik DT, Tian L, Lee J, Sayed N, Chen IY, Rhee S, Rhee JW, Kim Y, Wirka RC, Buikema JW, et al. Large-scale single-cell RNA-Seq reveals molecular signatures of heterogeneous populations of human induced pluripotent stem cell-derived endothelial cells. *Circ Res*. 2018;123:443–450. doi: 10.1161/CIRCRESAHA.118.312913
43. Chistiakov DA, Orekhov AN, Bobryshev YV. Effects of shear stress on endothelial cells: go with the flow. *Acta Physiol (Oxf)*. 2017;219:382–408. doi: 10.1111/apha.12725
44. Alsaffar H, Martino N, Garrett JP, Adam AP. Interleukin-6 promotes a sustained loss of endothelial barrier function via Janus kinase-mediated STAT3 phosphorylation and de novo protein synthesis. *Am J Physiol Cell Physiol*. 2018;314:C589–C602.
45. Marcos-Ramiro B, Garcia-Weber D, Millan J. TNF-induced endothelial barrier disruption: beyond actin and Rho. *Thromb Haemost*. 2014;112:1088–1102. doi: 10.1160/th14-04-0299
46. Stalker TJ, Welsh JD, Tomaiuolo M, Wu J, Colace TV, Diamond SL, Brass LF. A systems approach to hemostasis: 3. Thrombus consolidation regulates intrathrombus solute transport and local thrombin activity. *Blood*. 2014;124:1824–1831. doi: 10.1182/blood-2014-01-550319
47. Paschalaki KE, Starke RD, Hu Y, Mercado N, Margariti A, Gorgoulis VG, Randi AM, Barnes PJ. Dysfunction of endothelial progenitor cells from smokers and chronic obstructive pulmonary disease patients due to increased DNA damage and senescence. *Stem Cells*. 2013;31:2813–2826. doi: 10.1002/stem.1488
48. Smadja DM, Mauge L, Gaussem P, d'Audigier C, Israel-Biet D, Celermajer DS, Bonnet D, Levy M. Treprostinil increases the number and angiogenic potential of endothelial progenitor cells in children with pulmonary hypertension. *Angiogenesis*. 2011;14:17–27. doi: 10.1007/s10456-010-9192-y
49. Starke RD, Ferraro F, Paschalaki KE, Dryden NH, McKinnon TAJ, Sutton RE, Payne EM, Haskard DO, Hughes AD, Cutler DF, et al. Endothelial von willebrand factor regulates angiogenesis. *Blood*. 2011;117:1071–1080. doi: 10.1182/blood-2010-01-264507
50. Starke RD, Paschalaki KE, Dyer CE, Harrison-Lavoie KJ, Cutler JA, McKinnon TA, Millar CM, Cutler DF, Laffan MA, Randi AM. Cellular and molecular basis of von Willebrand disease: studies on blood outgrowth endothelial cells. *Blood*. 2013;121:2773–2784. doi: 10.1182/blood-2012-06-435727
51. Smadja DM, Melero-Martin JM, Eikenboom J, Bowman M, Sabatier F, Randi AM. Standardization of methods to quantify and culture endothelial colony-forming cells derived from peripheral blood: position paper from the international society on thrombosis and haemostasis ssc. *J Thromb Haemost*. 2019;17:1190–1194. doi: 10.1111/jth.14462
52. Chang TY, Tsai WC, Huang TS, Su SH, Chang CY, Ma HY, Wu CH, Yang CY, Lin CH, Huang PH, et al. Dysregulation of endothelial colony-forming cell function by a negative feedback loop of circulating miR-146a and -146b in cardiovascular disease patients. *PLoS One*. 2017;12:e0181562. doi: 10.1371/journal.pone.0181562

Supplemental Material

Table S1. Number of sequenced reads for all cell types.

Cell type	Number of sequenced reads
HUVEC	43160124
	35206048
	33724560
	43989327
iEC	40995771
	42608116
	36426081
	38279743
BOEC	38459193
	32729762
	37861169
	38260479

Figure S1. Assessment of iECs vessel formation through vasculogenesis-chip.

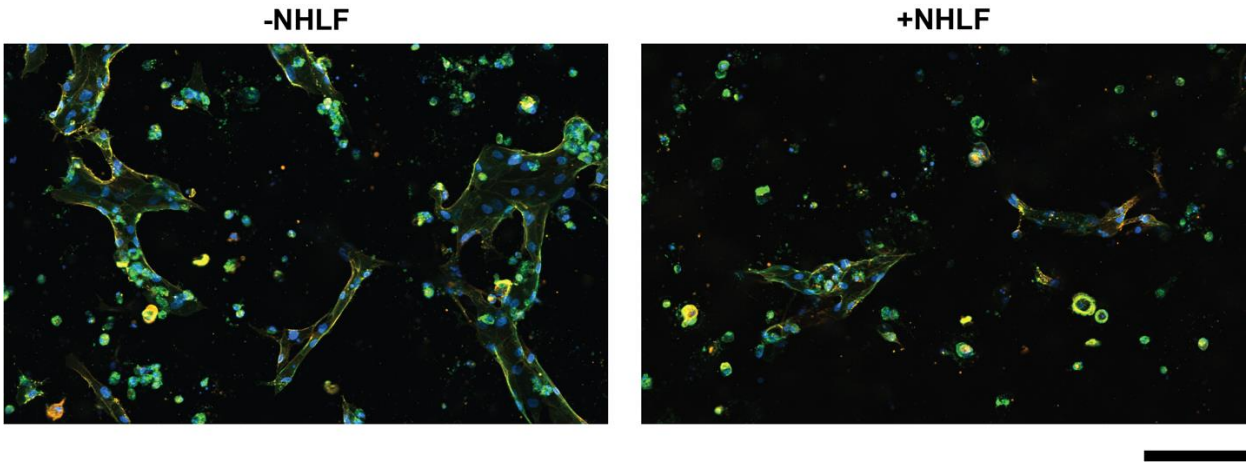

iECs were unable to form confluent networks, both with and without fibroblasts (scale bar: 200 μm).

Figure S2. Qualitative assessment of differentially expressed genes.

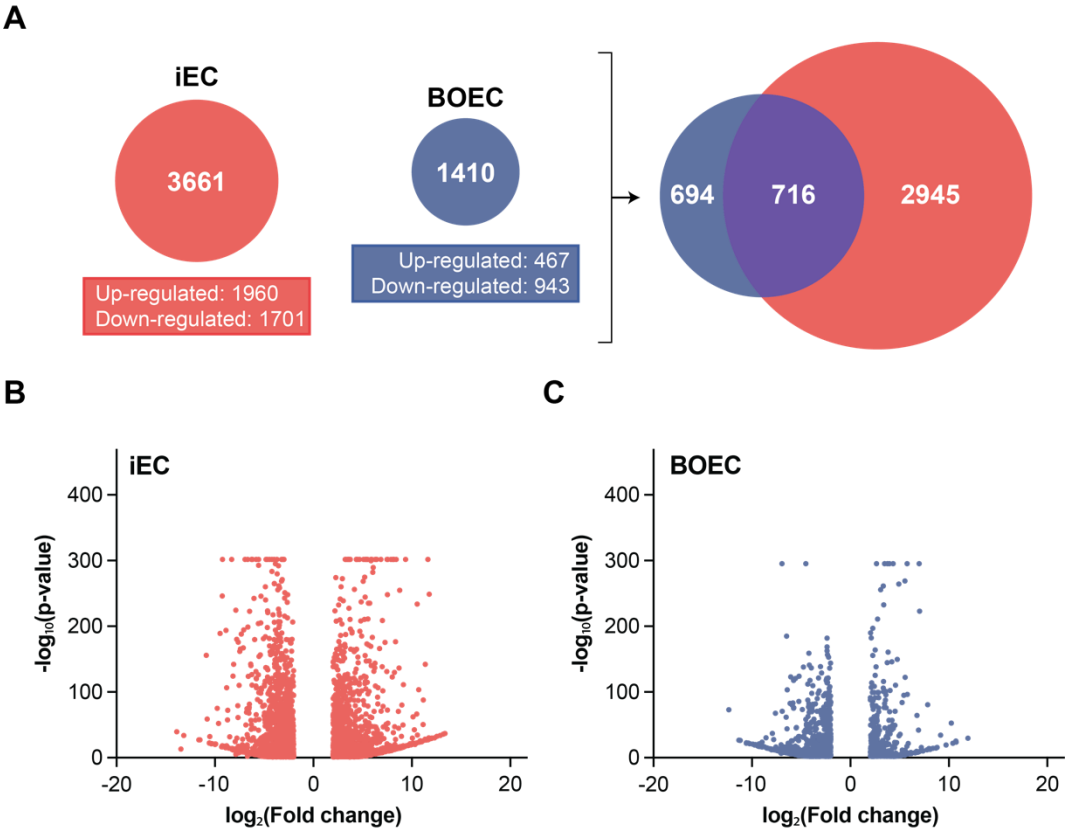

(A) Differential gene expression analysis revealed significant differences in the number of differentially expressed genes between iECs and BOECs when compared w.r.t. HUVECs; iECs expressed significantly more genes compared to BOECs. Out of the ~3600 genes expressed by iECs and ~1400 genes expressed by BOECs, ~700 genes were commonly expressed by the two cell types. **(B** and **C)** Volcano plots of differentially expressed genes for iECs and BOECs respectively relative to HUVECs. In agreement with (B), iECs exhibit a higher number of expressed genes relative to HUVECs as compared to BOECs. iECs had a higher and statistically stronger fold change differences compared to BOECs. Genes with $\log_2$(fold change) values between -2 and 2 were not considered differentially expressed and removed from the analysis.

Figure S3. Assessment of iECs lumen integrity using vessel-chip.

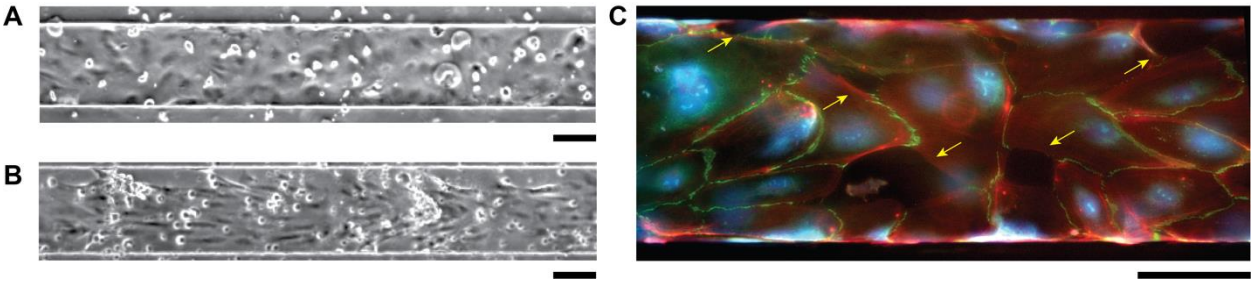

(A) Brightfield image of iECs showing initial attachment (t=0 hr, scale bar: 100 μm). **(B)** Brightfield image of iECs after 24 hours of culture in the vessel-chip (scale bar: 100 μm). **(C)** Fluorescence micrograph of iECs after 48 hours of perfusion culture (red: F-actin, green: VE cadherin, blue: nuclei; scale bar: 100 μm). Arrows depict areas where iEC lumen had large gaps.